# ASSESSMENT OF NUMERICAL MODELS TO REPRESENT THE LAMINATED ROTOR CORE OF ELECTRICAL MACHINES

**Hideraldo L. V. dos Santos, hideraldos@weg.net**
WEG Equipamentos Elétricos S.A. – Rua Waldemar Grubba, 3000, Jaraguá do Sul , SC, Brazil

**Carlos Alberto Bavastri, bavastri@ufpr.br**
Universidade Federal do Paraná (UFPR) – Rua General Carneiro, 370, Curitiba, PR, Brazil

**Marco Antônio Luersen, luersen@utfpr.edu.br**
Universidade Tecnológica Federal do Paraná (UTFPR) – Av. Sete de Setembro, 3165, Curitiba, PR, Brazil

***Abstract.*** *Almost all rotating electrical machines have rotors that are composed of a metallic cylinder and a steel shaft assembled with interference fit. This cylinder is made up of a compacted stack of thin metallic plates, usually referred to as laminated core. The laminated type structure is necessary in order to improve the electrical performance of the machine. On the other hand it enhances the stiffness of the system and an inadequate characterization of this element may lead to huge errors in the assessment of the dynamic behavior of the rotor. In face of this fact, the purpose of the present work is to compare and evaluate three beam models which allow the representation of the stiffening effect of the laminated core on the dynamic behavior of the rotating electrical machine rotor. Towards this end, a literature review is firstly carried out and three equivalent beam models using finite elements are selected and implemented, namely (i) "equivalent diameter model", (ii) "unbranched model" and (iii) "branched model". With the objective of validating the models, a set of experiments is then performed with nine different rotors of electrical machines, so that the first natural frequencies and the corresponding vibration modes in a free-free support condition could be obtained in practice. The models are evaluated by comparison of the natural frequencies and corresponding mode shapes obtained by the experimental analysis with those obtained by numerical analysis. The results show that, for the majority of the tested rotors, the branched model is the most suitable one. Finally, a critical discussion about the behavior of the equivalent beam models studied is presented.*

***Keywords****: rotordynamics, equivalent beam model, electrical machines, natural frequencies*

## 1. INTRODUCTION

During the design of an electrical machine, all its functional requirements must be established in order to ensure its durability, reliability, performance and environmental acceptability. The majority of those requisites are inextricably linked to the vibration behavior of the machine, and usually are the concern of international standards (Ehrich, 2004). While the actual knowledge in rotordynamics concepts allowed a big progress in the design of rotating machines to satisfy those standards, some important features are still missing in their development. An example is the development of models for rotors with laminated core used in electrical machines, where the problem is to determine how much stiffness this core adds to the shaft according to the type of the rotor's construction (Santos, 2008). The API 684 (2005) standard is a tutorial intended to describe, discuss, and clarify the API Standard Paragraphs which outlines the lateral and torsional rotordynamics analysis. According to this document we can use an equivalent beam model to represent the laminated rotor core of the electrical machines, and the stiffness effect can be simulated increasing the shaft diameter at the stack region. A recommendation about an approximated method to know how much will be the new shaft diameter is to calculate an equivalent diameter such that the additional mass is the same as the mass of the laminated core.

In Kim and Kim (2006) is shown the results of a numerical-experimental study about the relationship between the lamination pressure used to compose the core and the equivalent diameter of the beam model in order to consider the lamination stiffness effect. The authors used as a test rig a 642kg rotor composed just by the shaft and the laminate, without slots for the squirrel cage bars. As a conclusion, the author recommended to increase the shaft diameter at core region from 17 to 23% of the value of the difference between outer and inner core diameters. The results were based on a experiment that get the first thirtieths natural frequencies and correspondent mode shapes of the rotor tested, in a free-free condition. The modal analysis was repeated many times for different lamination pressures and the behavior of natural frequencies was obtained for each condition. The authors noticed an increment in the natural frequencies' values according to increment in the lamination pressure. This increment was not directly proportional to the pressure value and for high lamination pressures, the natural frequencies do not change significantly. Chen *et al.* (2008) did a wider proposal in order to modeling the entire electrical machine. To represent the laminated core, they used a dual rotor arrangement with the shaft and laminated elements connected by springs with stiffness around $10^9$N/m. The material properties of the rotor that represent the laminated core were experimentally fitted using the free-free natural frequencies of the rotor. The Young's modulus for the shaft and laminates were found to be 225GPa and 15GPa respectively, and 88GPa and 6GPa for the shear modulus. Garvey *et al.* (2004) suggested modeling the laminated core as an orthotropic material via a new definition of stress-strain state that considers the flexibility between the sheets of

the core. Two configurations were investigated. In the first one, namely "unbranched model", the shaft and the core elements are joined in parallel connecting to each other in the both ends in a common node. In the second one, namely "branched model", it was use a dual rotor with the elements connected by a spring and a damper, like the work of Chen *et al.* (2008).

To summarize, the equivalent beam models from literature uses a parameter to determine the stiffening effect of the laminate on the shaft. In most cases, this parameter must be fitted experimentally and is restricted to a specific rotor used as test rig, as shown for example in Garvey *et al.* (2004). Moreover, for different natural frequency mode shapes, the authors verified a considerable change in the value of the model's parameter for the same rotor. Based on this context, the first intention of this work is to answer the following question: "Is it possible to represent different squirrel cage rotors geometries and different modes shape using only one equivalent beam model with only one parameter's value for all modes?"

The approach used here was to evaluate the following three versions of equivalent beam models: (i) using an equivalent shaft diameter in the core region, namely "equivalent diameter model", (ii) using a finite element to represent separately the laminated core and another to represent the shaft, connecting the ends of the elements in a same node, this case namely "unbranched model" and (iii) the same idea from (ii), but the ends of the shaft and laminated elements connected by springs, for that reason it is named "branched model". These models are described in Section 2. Then, the main objective of this work is to implement the three equivalent beam models using the finite element method and to carry out experiments for evaluating the behavior of the models for different squirrel cage rotors geometries.

## 2. MODELS DESCRIPTION

### 2.1. Model 01: equivalent diameter

The most common manner for modeling the laminated core is to use a value of equivalent shaft diameter in the core region. In this way, the laminated core is considered as a part of the shaft, adding beyond mass and inertia, a contribution in the total stiffness of the rotor (Kim and Kim, 2006). The rotor is composed by an assembled cylinder of stacked sheets with total length $L_{CH}$, diameter $\phi_{CH}$ and mass $M_{CH}$, including the rotor bars (see Fig. 1a). The end ring has length $L_{AC}$, outer diameter $\phi_{AC}$ and mass $M_{AC}$. The shaft diameter $\phi_E$ at the core position is added by a value $\Delta\phi_E$ (Fig. 1b). The new diameter in the core region is referred as $\phi_{EQV}$, and given by

$$\phi_{EQV} = \phi_E \left(1 + pt\right) \tag{1}$$

where *pt* means the relative increase applied to the shaft base diameter and varies from 0 to 1 which means 0% to 100% of the original shaft diameter. The remaining laminated part, the outer core diameter minus $\phi_{EQV,}$ is divided equally in *N* discs. Each disc has inner diameter equals to $\phi_{EQV}$ and outer diameter equals to the core outer diameter in order to maintain the original inertia of laminate and the mass of each disc are properly calculated to maintain the total mass of the rotor. This assemble is converted into an equivalent beam system with mass and inertia concentrated in the of the core region (Fig. 1c).

Using the concepts described above, the only unknown parameter or model variable is *pt*, which defines the equivalent diameter in the core region. The others model parameters can be taken directly from the rotor geometry. Kim and Kim (2006) used two ways for analyzing the *pt* values: the first one was like the method described in Eq. 1, where the authors verified experimentally a variation from 0.28 to 0.36 in *pt*; in the second one the equivalent diameter is calculated using more information about the rotor's geometry, so that

$$\phi_{EQV} = \phi_E + \left(\phi_{CH} - \phi_E\right) pt \tag{2}$$

and, with this definition the authors verified that *pt* varies from 0.17 to 0.23. In both cases *pt* change for each rotor's natural mode shape.

Using the recommendations of API 684 (2005), the diameter increase must preserve the total mass of the laminated core $M_{CH}$, so that

$$\rho_E \; L_{CH} \frac{\pi\left(\phi_{EQV}{}^2 - \phi_E{}^2\right)}{4} = M_{CH} \tag{3}$$

where

$$\phi_{EQV} = \sqrt{\frac{4M_{CH}}{\pi\rho_E \; L_{CH}} + \phi_E{}^2} \tag{4}$$

In this case, $\phi_{EQV}$ can not be written down as a function of *pt* and the result diameter need to be compared directly.

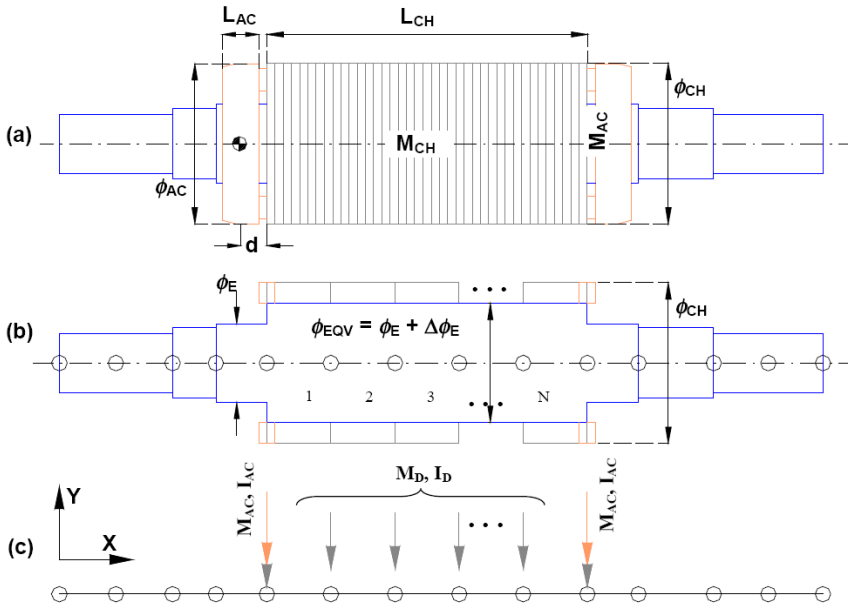


Figure 1. Sequence for representing the laminated core by an equivalent diameter of she shaft. (a) solid model (b) equivalent solid model (c) equivalent beam model.

### 2.2. Model 02: unbranched model

In this aproach, the laminated stack is modeled as a continuous tube with equivalent elastic properties in order to simulate its compliance (Garvey *et al.*, 2004). Supposing that the cylinder is assembled with interference on the shaft, it results in a compound section with two materials (Fig. 2b, section A-A). To convert this system to a finite element model, we used two beam elements in parallel in the core region, one for the shaft and another for the core (Fig. 2c). For both elements the Timoshenko beam model with isotropic material were used, although Garvey *et al.* (2004) suggested a new formulation for the elements of the laminates, based on an orthotropic equivalent material formulation. In this case, the lamination compliance is simulated changing the material's Young modulus *E_pct*, just for the laminated cylinder elements. Using the conception described above, the only one unknown parameter or model variable is the *E_pct* for the core region, the other model parameters can be obtained directly from the rotor geometry.

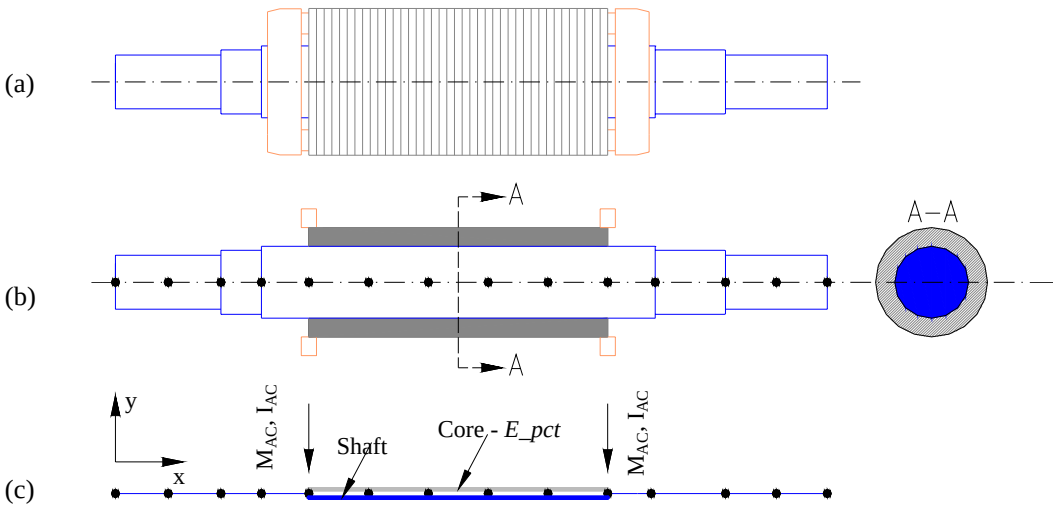


Figure 2. Schematic diagram of lamination stack represented as a parallel beam (unbranched model).

### 2.3. Model 03: branched model

In the branched model, the lamination core is modeled as a continuous cylinder with same isotropic elastic properties of the shaft and it is connected to the shaft by a flexible interface (springs), looking like a dual rotor system. Converting to a finite element model, the laminated elements are attached to the shaft elements (both using Timoshenko beam theory) node to node by springs with total a stiffness *Kc* (Fig. 3b). The stiffening effect of laminate is represented here just by the value of the *Kc*, so that *Kc* is the only unknown parameter or model variable of this model.

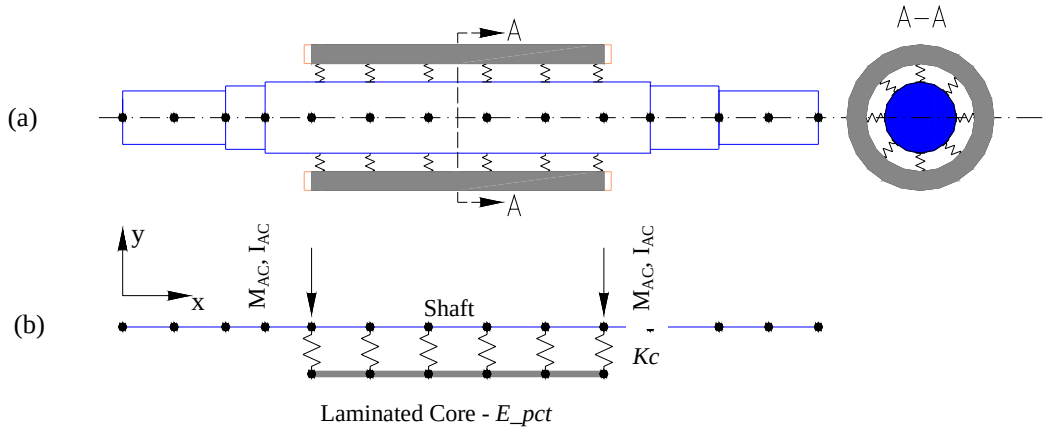


Figure 3: Arrangement for the branched model as a dual rotor.

### 2.4. Implementation

The three models described above were implemented in the commercial finite element software ANSYS rev. 11.0. A macro was developed in APDL language in order to build a parametric model for an easy post-analysis. The basic data used for the rotor were: the shaft steps lengths, the shaft steps outer and inner diameters, the Young's modulus, the Poisson's ratio and density for the shaft material and the total lamination core mass. Three finite element types were used to represent the system: Timoshenko beam element of class $C^1$ for the shaft and for the laminated core in the Models 02 and 03; point mass element (with mass and inertia moments) to represent the discs in Model 01 and one-dimensional spring element to represent the interface between the shaft and the laminated core in the Model 03.

The discrete system is written in a matrix form represented by the equations of motion, so that, in the free motion may be expressed as

$$[\mathbf{M}]\ \{\ddot{\mathbf{q}}(t)\}+([\mathbf{C}]+[\mathbf{G}])\{\dot{\mathbf{q}}(t)\}+[\mathbf{K}]\ \{\mathbf{q}(t)\}=\{\mathbf{0}\} \tag{5}$$

where $[\mathbf{M}]$ is the mass matrix, $[\mathbf{K}]$ is the stiffness matrix, $[\mathbf{C}]$ is the damping matrix, $[\mathbf{G}]$ is the gyroscopic matrix, $\{\mathbf{q}(t)\}$ is the nodal displacement vector, $\{\dot{\mathbf{q}}(t)\}$ is the nodal velocity vector and $\{\ddot{\mathbf{q}}(t)\}$ is the nodal acceleration vector.

## 3. EXPERIMENTAL MODAL ANALISYS

The purpose of the experiments carried out in this work was to obtain the modals parameters (natural frequencies and mode shapes) of samples of different building characteristics of squirrel cage rotors. The results of these experiments were used to evaluate the performance of the three equivalent beam models implemented.

### 3.1. Rotors tested

No prototype was developed specifically for the tests. They were performed using rotors commercially available from WEG Company, with no control of the interference between the rotor core and the shaft. Table 1 briefly describes some of the features of the rotors tested. The samples were selected aiming to include the most common types of squirrel-cage rotors used in electrical machines.

Table 2 presents some of the geometric ratios of the rotors tested. The ratio between the length of the core and the length of the shaft ($L_{CH}/L_{SHAFT}$) , the ratio between the diameter of the plates of the core and the diameter of the shaft in the core region ($\phi_{CH}/\phi_E$), the ratio between the diameter of the yoke of the plate of the rotor and the diameter of the shaft in the core region ($\phi_{CO}/\phi_E$), the ratio between the height of the yoke of the plate of the rotor and the radius of the shaft in

the core region ($H_{CO}/R_E$), the ratio between the total mass of the core and the mass of the shaft ($M_T/M_{SHAFT}$), the ratio between the length of the core and diameter of the plates of the core ($L_{CH}/\phi_{CH}$), the ratio between the length of the core and the diameter of the yoke of the plates of the core ($L_{CH}/\phi_{CO}$).

Table 1. Some characteristics of the tested rotors.

| Designation[1] | Mass (kg) | Description |
|---|---|---|
| 225IIP | 70.0 | Rotors with continuous aluminum bars, without ventilation channels (continuous core) |
| 250IVP | 141.0 | |
| 355IIP(A) | 355.0 | |
| 355IIP(B) | 367.0 | |
| 355IIP(C) | 378.0 | |
| 315IIP | 389.0 | Rotors with aluminum bars and axial ventilation channels (continuous core) |
| 400IIP | 828.0 | Rotors with copper bars and axial ventilation channels (continuous core) |
| 450IVP | 1224.0 | |
| 560IIP | 1890.0 | Rotors with copper bars and axial and radial ventilation channels (spaced cores) |

Table 2. Geometric relations of the tested rotors.

| Rotor's designation | $\frac{L_{CH}}{L_{SHAFT}}$ | $\frac{\phi_{CH}}{\phi_E}$ | $\frac{\phi_{CO}}{\phi_E}$ | $\frac{H_{CO}}{R_E}$ | $\frac{M_T}{M_{SHAFT}}$ | $\frac{L_{CH}}{\phi_{CH}}$ | $\frac{L_{CH}}{\phi_{CO}}$ |
|---|---|---|---|---|---|---|---|
| 225IIP | 0.24 | 2.58 | 1.56 | 0.56 | 1.32 | 0.86 | 2.82 |
| 250IVP | 0.37 | 3.05 | 2.20 | 1.20 | 3.01 | 1.27 | 3.78 |
| 355IIP(A) | 0.33 | 3.18 | 2.03 | 1.03 | 2.97 | 1.29 | 3.75 |
| 355IIP(B) | 0.33 | 2.87 | 1.83 | 0.83 | 2.52 | 1.29 | 3.95 |
| 355IIP(C) | 0.33 | 2.41 | 1.54 | 0.54 | 1.76 | 1.29 | 4.39 |
| 315IIP | 0.31 | 2.21 | 1.68 | 0.68 | 1.42 | 0.00 | 6.17 |
| 400IIP | 0.28 | 1.80 | 1.40 | 0.40 | 0.87 | 1.65 | 7.44 |
| 450IVP | 0.31 | 2.07 | 1.67 | 0.67 | 1.21 | 1.87 | 7.25 |
| 560IIP | 0.31 | 2.04 | 1.57 | 0.57 | 1.20 | 2.12 | 8.33 |

### 3.2. Description of the experiments

All the rotors were tested in the "free-free" condition. Figure 4 shows the 560IIP rotor, which weighs approximately 2 tonnes, suspended by slings and a a hoist. Data acquisition was performed using an analyzer with four channels from Brüel & Kjaer, Pulse Data Acquisition 3560C model. The excitation was carried out using instrumented hammers from ENDEVCO, model 2203-5 (for the 225IIP and 250IVP rotors) and model 8208 (for the rest of the rotors) [2] . The vibration peak was measured with a TEDS accelerometer, model 752A12, also from ENDEVCO.

The rotors were discretized as shown in Fig. 5 for the rotor 560IIP. The excitation was carried out using a modal hammer in a point in the front drive of the shaft while the accelerometer pass trough measuring the response on the other points. This guaranteed that the first vibration modes were obtained sequentially because in the extremities of the beam (the rotor) never will be a node for the boundary conditions tested. The software used for the data acquisition, with a FRF curve (frequency response function) and coherence was PulseLabshop and the modal analysis software was ME'scopeVES. In all measurements were used 10 averages to compose the FRF with a resolution of 1Hz. In average, the frequency bandwidth was from 10Hz to 5kHz. The signals were obtained using a uniform window for the hammer force, and an exponential window for the response from the accelerometer.

[1] The first three numbers are associated to rotor size. The next two numbers in roman numbers are associated to the number of poles / rotor rotation (for example, IIP is a 3600rpm rotor speed and IVP an 1800rpm one).
[2] The type of the hammer used is directly associated to the mass of the rotor being tested. a certain mass, it was necessary to use the 8208 hammer which is suitable for heavy structures.

Figure 4. Rotor suspended for a free-free support condition experimental test.

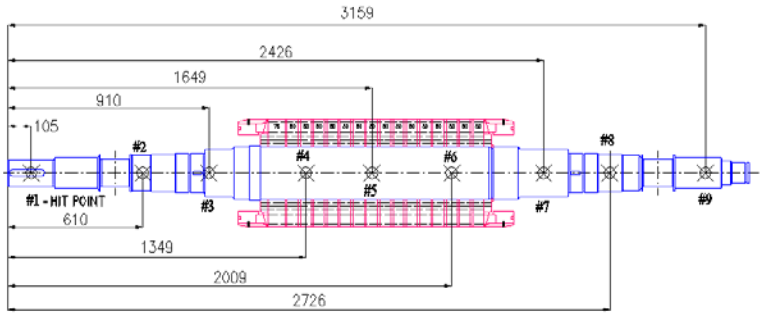


Figure 5. Excitation and response point positions (in mm).

### 3.3. Modal parameters extraction

The techniques of obtaining the inertance curves from the modal analysis were based on Ewins (1984). The modal parameters were extracted in the frequency domain, using all the inertance curves of the degrees of freedom (discrete measurement points) simultaneously. To estimate the modal parameters the minimum least square method was used (ME'scopeVES, 2003). Table 3 presents a summary of the natural frequency values obtained experimentally for each rotor. The number of modes obtained for each rotor was defined by the frequency band in which it was possible to maintain the excitation of the modal hammer relatively constant (deviation smaller than 3dB). For this reason, for some rotors, it was possible to obtain four modes, while for others, only three were obtained. Although obtained experimentally, modal damping was neglected, as none of the models presented in this paper include this effect.

Table 3. Experimental natural frequencies for each rotor (in Hz).

| Rotor | Freq. #1 | Freq. #2 | Freq. #3 | Freq. #4 |
|---|---|---|---|---|
| 225IIP | 688 | 1203 | 2597 | 3039 |
| 250IVP | 612 | 928 | 2169 | 2794 |
| 355IIP(A) | 329 | 579 | 1290 | - |
| 355IIP(B) | 395 | 683 | 1362 | - |
| 355IIP(C) | 468 | 822 | 1384 | - |
| 315IIP | 332 | 493 | 853 | 1140 |
| 400IIP | 288 | 454 | 711 | - |
| 450IVP | 167 | 302 | 527 | 710 |
| 560IIP | 137 | 202 | 429 | 566 |

## 4. RESULTS COMPARISON

### 4.1. Numerical-experimental error of the models

To evaluate the proposed beam models their parameters were varied within a pre-established range. The first natural frequencies with their corresponding modes of vibration were then calculated. These frequencies and modes were compared to those obtained experimentally, in order to determine the percentual errors in the natural frequency

calculation values in relation to the experimental values, for each model parameter value. This was done for each of the rotors and each beam model. Figures 7, 8 and 9 show the calculated errors for the 225IIP rotor. For each rotor and model, the error was plot in a graph, as shown in Figs. 7, 8 and 9 for the 225IIP rotor. The lines with markers correspond to the variation (absolute value) of the error of each first natural frequency, while the solid line (in red) represents the average error as a function of the parameter used in each model.

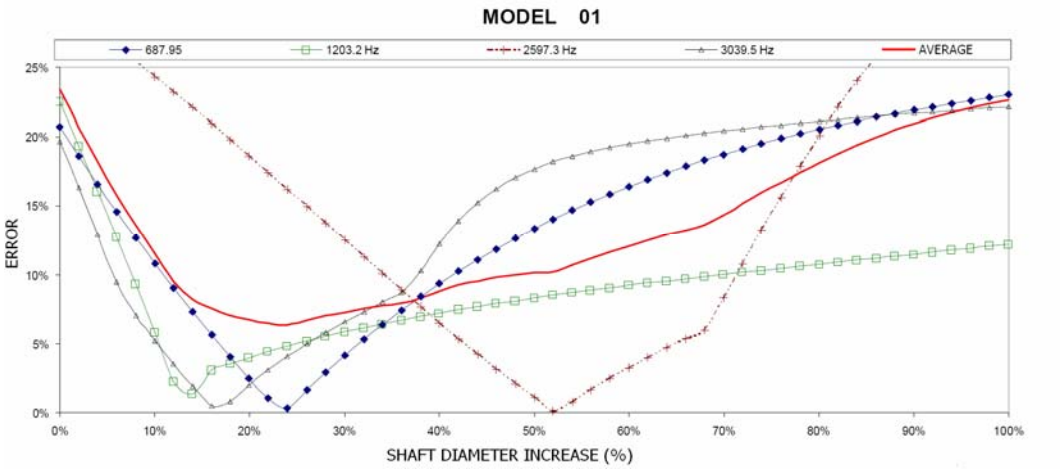


Figure 7 Error in the natural frequencies for rotor 225IIP – Model 01.

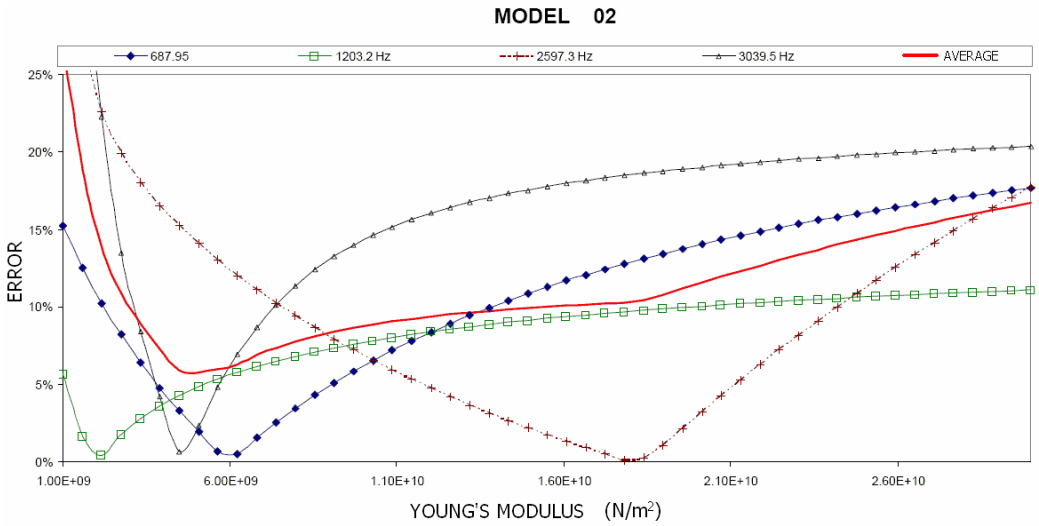


Figure 8. Error in the natural frequencies for rotor 225IIP – Model 02.

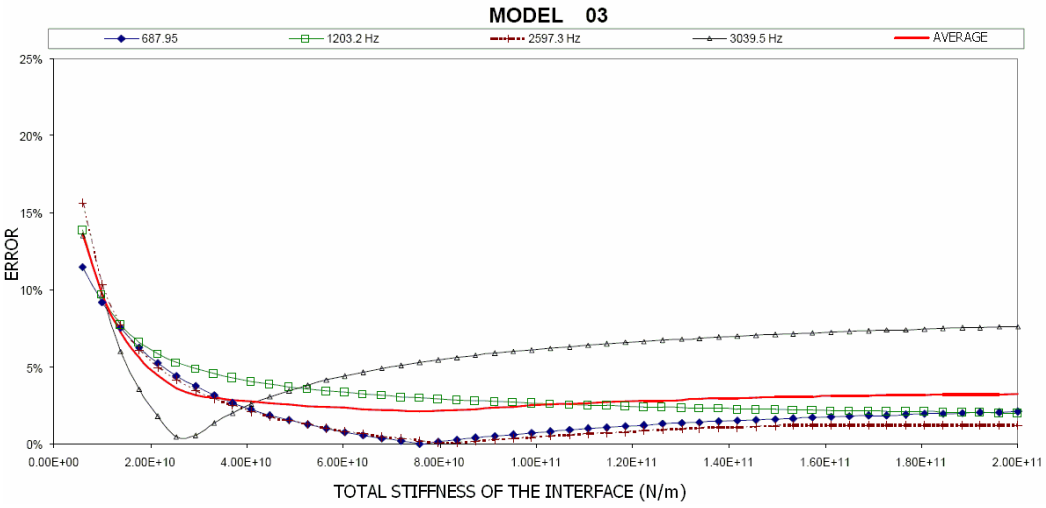


Error in the natural frequencies of rotor 225IIP – Model 03.

Figure 10 shows an example of comparison of the vibration modes obtained experimentally and numerically by the three models in the minimum error condition for the 355IIP(A) rotor. Despite the modal damping was obtained experimentally, it was neglected in the numerical models.

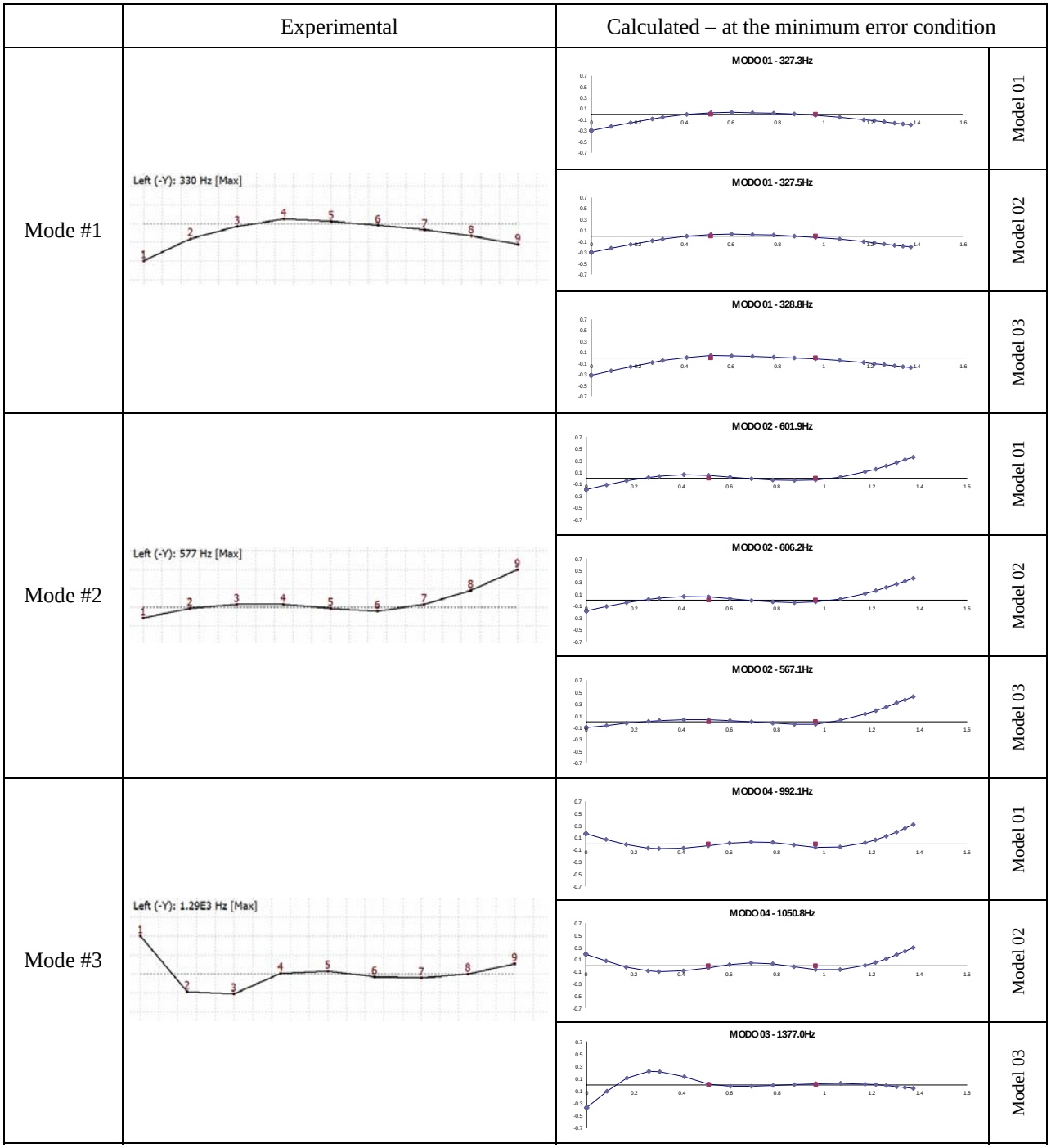


Figure 10. Comparison of the mode shapes for 355IIP(A) rotor.

### 4.2. Models' accuracy

The graphs of the Figs. 7, 8 and 9 show many points that minimize the numerically error, fitting exactly the natural frequencies for each rotor mode shape in different values of parameters. This indicates that the stiffness effect changes for each mode when we use equivalent beam models to represent the rotors with laminated core. In an ideal model, we should expect to use a same model's parameter to reproduce all the dynamic characteristics of rotor. Then, to evaluate how much the equivalent beam model is approximating to the ideal model we proposed the follow idea: *How less*

*dispersal the values of parameters that minimize the error in each mode shape, more accurate will be the equivalent model for a given rotor.*

Based on the graphs above, we can use the average error curve in order to get the accuracy information. Therefore, the accuracy of the equivalent model will be determined by the value of minimum average error that, from now on, will be namely just as minimum error. Then, how much small is the minimum error, more accurate is the model. Table 4 shows a summary of minimum error obtained for each model in each rotor tested and the number of modes considered for each rotor. According to these results, Model 03 points out as the most accurate in almost all rotors tested (6 of the 9). Additionally, we can infer that Models 01 and 02 can be considered as equivalent concerning to their accuracy. This conclusion was reported in Garvey *et al*. (2004), confirming that the Model 03 arrangements is the best model, among the ones implemented, to represent the rotors with a laminated core.

Table 4. Minimum error in the natural frequencies for each equivalent beam model.

| Rotors | Model 01 | Model 02 | Model 03 | N. of modes |
|---|---|---|---|---|
| 225IIP | 6.4% | 5.8% | 2.1% | 04 |
| 250IVP | 12.5% | 10.2% | 6.0% | 04 |
| 355IIP(A) | 9.2% | 8.5% | 1.9% | 03 |
| 355IIP(B) | 6.8% | 6.1% | 1.8% | 03 |
| 355IIP(C) | 2.7% | 2.6% | 1.2% | 03 |
| 315IIP | 3.1% | 2.3% | 3.7% | 04 |
| 400IIP | 1.9% | 1.7% | 0.3% | 03 |
| 450IVP | 3.0% | 2.1% | 4.4% | 04 |
| 560IIP | 3.6% | 3.2% | 4.0% | 04 |

The final purpose is to know if a single equivalent beam model can be used to represent different rotors geometries without the requirement of identifying experimentally the models parameters for each case. The information of model's accuracy is not sufficient to evaluate this characteristic, it is necessary to determine the robustness of the model. So, the next Sub-Section describes the second criteria to evaluate the equivalent beam model.

### 4.3. Evaluation of the models' robustness

Table 5 shows the correspondent parameter for minimum error condition of Tab. 4 in each model. The average of the parameters of each rotor is used as a fixed value to recalculate the natural frequencies. The new average error values for the *N* first natural frequencies are shows in Tab. 6. I can be noticed that Model 03 keeps the average error below 5% using only one value for the model's parameter in almost all rotors tested (7 of the 9). The exceptions were the rotors 250IVP and 450IVP.

Table 5. Models' parameter values for the minimum error for each rotor.

| Rotor | Model 01<br>*pt (%)* | Model 02<br>*E_pct* (GPa) | Model 03<br>*Kc* (N/m) |
|---|---|---|---|
| 225IIP | 23.9% | 5.1 | $7.6 \times 10^{10}$ |
| 250IVP | 55.2% | 14.0 | $9.9 \times 10^{09}$ |
| 355IIP(A) | 42.4% | 6.2 | $5.6 \times 10^{10}$ |
| 355IIP(B) | 45.6% | 9.7 | $1.7 \times 10^{11}$ |
| 355IIP(C) | 29.6% | 10.0 | $4.9 \times 10^{10}$ |
| 315IIP | 30.0% | 17.0 | $3.3 \times 10^{10}$ |
| 400IIP | 15.6% | 16.0 | $1.8 \times 10^{10}$ |
| 450IVP | 10.0% | 6.2 | $1.1 \times 10^{10}$ |
| 560IIP | 28.8% | 21.0 | $4.1 \times 10^{10}$ |
| Average | 31.2% | 12.0 | $5.1 \times 10^{10}$ |

Table 6. Average error in the natural frequencies for the *n* first natural frequencies with fixed parameter.

| Rotor | Model 01 | Model 02 | Model 03 |
|---|---|---|---|
| 225IIP | 7.4% | 9.3% | 2.4% |
| 250IVP | 20.1% | 11.5% | 9.7% |
| 355IIP(A) | 15.% | 10.6% | 2.1% |
| 355IIP(B) | 13.5% | 6.7% | 2.8% |
| 355IIP(C) | 3.2% | 3.3% | 1.3% |
| 315IIP | 3.3% | 4.5% | 4.0% |
| 400IIP | 6.7% | 2.5% | 3.4% |
| 450IVP | 16.1% | 5.8% | 13.3% |
| 560IIP | 3.8% | 5.7% | 4.2% |

## 5. CONCLUSION

In this work, three beam models to represent the laminated core of electrical machine rotors were implemented and evaluated. The approach chosen to evaluate them was comparing the natural frequencies and mode shapes obtained numerically and experimentally. Nine specimens of squirrel-cage rotors were used for the experiments. As each model has a variable parameter, it was found out that, to fit the numerical and experimental results, the model parameter is dependent on the mode considered. For each model, choosing only one parameter value to represent all the rotors and all the modes, Model 03 (the "branched model") was the most robust for almost all rotors tested. Exception to this deviations, with the Model 03 it was possible to calculate the three first natural frequencies of all rotors with an error less than 5%, using only one value for the parameter.

## 6. ACKNOWLEDGEMENTS

The authors would like to thank MCT-FINEP under the project PROMOVE 4931/06 and WEG Company for the financial support.

## 7. REFERENCES

API 684 - American Petroleum Institute Standards, 2005, "API Recommended Practice 684: Rotordynamics tutorial - lateral critical speeds, unbalance response, stability, train torsionals, and rotor balancing", Washington, D.C.

Bordalo, S.N., Ferziger, J.H. and Kline, S.J.,1989, "The Development of Zonal Models for Turbulence", Proceedings of the 10th Brazilian Congress of Mechanical Engineering, Vol.1, Rio de Janeiro, Brazil, pp. 41-44.

Chen, Y. S., Cheng, Y. D., Liao, J. J. and Chiou, C. C., 2004, "Development of a finite element solution module for the analysis of the dynamic behavior and balancing effects of an induction motor system", Finite Elements in Analysis and Design, Vol.44, pp. 483-492.

Ehrich, F.F., 2004, "Handbook of Rotordynamics", 3. ed. Florida: Krieger Publishing Company.

Ewins, D.J., 1984, "Modal Testing: Theory and Practice", 1a. ed., Great Britain: Research Studies Press Ltd.

Garvey, S.D., Penny, J. E. T., Friswell, M. I. and Lees, A. W., 2004, "The Stiffening Effect of Laminated Rotor Cores on Flexible-Rotor Electrical Machines", In: IMECHE - International Conference on Vibrations in Rotating Machinery, Swansea, UK, pp. 193-202.

Kim, Y. C. and Kim, K. W., 2006, "Influence of lamination pressure upon the stiffness of laminated rotor", JSME International Journal, Vol. 49, No. 2, pp. 426-431.

Lalanne, M. and Ferraris, G., 1990, "Rotordynamics Prediction in Engineering", 1a. Ed., England, John Wiley & Sons Ltd.

ME'scopeVES Version 4.0.0.6, 2003, "Operating Manual: Volume II", Reference. Vibrant Technology, Inc.

Santos, H. L. V. dos, 2008, "Assessment of numerical models to represent the laminated rotor core of electrical machines", Master's Dissertation, Post Graduation Program in Mechanical and Materials Engineering, Federal Technological University of Paraná (UTFPR), Curitiba, 89p (in Portuguese).

## 8. RESPONSIBILITY NOTICE

The authors are the only responsible for the printed material included in this paper.